Highlights

Deep neural network method for predicting the iron concentration in silicon solar cell by current-voltage characteristic

Oleg Olikh,Oleg Lozitsky,Oleksii Zavhorodnii

- Research highlights item 1
- Research highlights item 2
- Research highlights item 3

Deep neural network method for predicting the iron concentration in silicon solar cell by current-voltage characteristic

Oleg Olikh[a,*], Oleg Lozitsky[a] and Oleksii Zavhorodnii[a]

[a]Taras Shevchenko National University of Kyiv, 64/13, Volodymyrska Street, City of Kyiv, Ukraine, 01601

ARTICLE INFO

Keywords:
Ideality factor
Silicon
n^+–p–p^+ structure
SCAPS
Iron contamination
Machine learning

ABSTRACT

Defect-assisted recombination processes frequently limit the photovoltaic device performance. Non–destructive methods of evaluation of the impurities contamination in solar cells, are important from an applied point of view. In this work, we use numerical device simulation to demonstrate the ability to extract impurity contamination from an ideality factor value and utilizing a deep neural network (DNN). The dense layer DNN was trained by using simulation of current-voltage curves of silicon n^+–p–p^+ structure with the following parameters. The iron concentration ranged from 10^{10} to 10^{13} cm^{-3}, the base doping level — from 10^{15} to 10^{17} cm^{-3}, the base thickness — from 150 to 240 micron, and the temperature — from 290 to 340 K. The structure with interstitial iron atoms only as well as with coexistence of Fe_iB_s pairs and Fe_i was under consideration. It is shown that DNN is able to predict iron concentration with mean squared relative error up to 0.03.

1. Introduction

Metal contamination control remains an important challenge for silicon processing both for microelectronics, logic technologies and solar cells (SCs) [2, 1, 3, 4]. Typically, metal related defect characterization is performed by Fourier-transform infrared spectroscopy, electron-paramagnetic resonance, minority carrier lifetime measurements, deep level transient spectroscopy (DLTS), Laplace DLTS etc [5, 6, 7]. However, these techniques are time-consuming, require special equipment or/and sample preparing. At the same time, the current-voltage (IV) measurement is a standard rapid industrial SC characterization technique. IV characteristics contain important information about electrically active defects [6, 8]. And a few defect diagnostics by IV characteristics are proposed [6, 8, 9, 10, 11]. The temperature dependencies of current components [10, 11] or IV differential parameters [8, 9] are under consideration. But the numerous and high accuracy IV measurements are required in the first and second cases, respectively.

In our previous work [12], we have shown that the SC ideality factor value (n) can be used to estimate the iron concentration (N_{Fe}). It should be noted that the ideality factor is quite often used to characterize the various semiconductor barrier structures [13, 14, 15, 16, 17]. However, a defect's signature in an ideality factor is convoluted with those from so many other physical processes. As a result the obtained analytic expressions $N_{Fe} = f(n)$ are not general and the numerous grading curves are needed to N_{Fe} determination [12]. On the other hand, in the last decade, the deep learning, which is enable to solve problems without clear algorithmization, have been successfully used in various fields of theoretical and applied physics [18, 19, 20]. Furthermore, materials informatics (combination of material property calculations/measurements and informatics algorithms) has been asserted [21] to become the fourth (along with theory, simulations, and experiments) paradigm of science. The aim of this work is to apply the deep learning approach for predicting the iron concentration from ideality factor (so to say "deep learning for deep levels"). Further, unlike in previous work [12], the back surface field (BSF) n^+–p–p^+ structure was under consideration and the base thickness influence on ideality factor was taken into account as well.

As the approximation to the practice on manufacturing line, the paper considers a fairly simple system which consists of crystalline silicon (c-Si) SC and iron impurity. However, the system is important in practice. Silicon solar cells constitute 90% of current global production capacity [**?**] and BSF is one of popular designs used for industrial

*Corresponding author
olegolikh@knu.ua (Oleg Olikh)
ORCID(s):

mass production of c-Si SCs [**?**]. Iron is a major as one of the most detrimental metal impurities in c-Si SCs [1, 3, 4].

$$E_G(T) = E_G(0) - \alpha\Theta\left\{\frac{1-3\Delta^2}{\exp\left(\frac{\Theta}{T}\right)-1} + \frac{3\Delta^2}{2}\left(\sqrt[6]{1+\frac{\pi^2}{3(1+\Delta^2)}\left(\frac{2T}{\Theta}\right)^2 + \frac{3\Delta^2-1}{4}\left(\frac{2T}{\Theta}\right)^3 + \frac{8}{3}\left(\frac{2T}{\Theta}\right)^4 + \left(\frac{2T}{\Theta}\right)^6} - 1\right)\right\}, \tag{1}$$

where $E_G(0) = 1.1701$ eV, $\alpha = 3.23 \times 10^{-4}$ eV/K, $\Theta = 446$ K, $\Delta = 0.51$.

$$\Delta E_G = 4.20 \times 10^{-5}\left[\ln\left(\frac{N_B}{10^{14}}\right)\right]^3; \qquad \Delta E_G = 4.72 \times 10^{-5}\left[\ln\left(\frac{N_A}{10^{14}}\right)\right]^3, \tag{2}$$

$$v_{\mathrm{th},n} = \sqrt{\frac{8qkT}{0.28m_0\pi}}; \qquad v_{\mathrm{th},p} = \sqrt{\frac{8qkT}{0.41m_0\pi}}, \tag{3}$$

where m_0 is the free electron mass.

$$\left(\frac{m^*_{dC}}{m_0}\right)^{1.5} = 1.094 - 1.312 \times 10^{-5}T + 6.753 \times 10^{-7}T^2 + 4.609 \times 10^{-10}T^3, \tag{4}$$

$$\left(\frac{m^*_{dV}}{m_0}\right)^{1.5} = 0.3426 + 3.376 \times 10^{-3}T - 4.689 \times 10^{-6}T^2 + 2.525 \times 10^{-9}T^3. \tag{5}$$

$$C_p(T) = (7.91 \times 10^{-32} - 4.13 \times 10^{-35}T + 3.59 \times 10^{-37}T^2) \times \left(1 + \left(564812T^{-1.6545} - 1\right)\left(1 - \tanh\left[\left\{\frac{p}{5 \times 10^{16}}\right\}^{0.29}\right]\right)\right), \tag{6}$$

$$C_n(T) = 2.8 \times 10^{-31} \times \left(1 + \left(235548T^{-1.5013} - 1\right)\left(1 - \tanh\left[\left\{\frac{n}{5 \times 10^{16}}\right\}^{0.34}\right]\right)\right). \tag{7}$$

This gives hope for an real implementation of aforesaid SC characterization method with using of deep learning approach (so to say "deep learning for deep levels").

studied relationship between the SC ideality factor and the iron concentration.

Any defects detrimental to the device performance should by definition have a signature in the device performance such as current–voltage (JV) measurements. However, such a signal is convoluted with those from so many other physical processes that it cannot be extracted or interpreted through a simple fitting approach, as the fit would be underconstrained.

The obtained results show that the ideality factor value can be used to estimate the contaminant concentration.

Non–destructive methods of evaluation of the impurities contamination in semiconductor structures, in particular solar cells (SCs), are important from an applied point of view. To date, a not little collection of direct methods (an infrared tomography, an electron-paramagnetic resonance, a non-stationary spectroscopy, etc.) as well as indirect methods (a surface photovoltage, a minority carrier lifetime measurements) has been developed to solve this problem. But almost all of them require special sample preparing or/and specialized equipment. At the same time, the current–voltage curve (IVC) measurement is a widespread industrial characterization technique and allows to determine a number of fundamental SC parameters. Evidently SC parameters in particular and the processes of carrier propagation in general depend on electrically active defects presence; therefore there is a possibility in principle to determine the impurity concentration by IVC shape. And recent papers demonstrate a novel approach to extract defect properties from inexpensive IV measurements of completed devices [6].

The Elsevier cas-sc class is based on the standard article class and supports almost all of the functionality of that class. In addition, it features commands and options to format the

- document style
- baselineskip
- front matter
- keywords and MSC codes
- theorems, definitions and proofs
- lables of enumerations
- citation style and labeling.

This class depends on the following packages for its proper functioning:

1. natbib.sty for citation processing;
2. geometry.sty for margin settings;
3. fleqn.clo for left aligned equations;
4. graphicx.sty for graphics inclusion;
5. hyperref.sty optional packages if hyperlinking is required in the document;

All the above packages are part of any standard LaTeX installation. Therefore, the users need not be bothered about downloading any extra packages.

2. Installation

The package is available at author resources page at Elsevier (`http://www.elsevier.com/locate/latex`). The class may be moved or copied to a place, usually, `$TEXMF/tex/latex/elsevier/`, or a folder which will be read by LaTeX during document compilation. The TeX file database needs updation after moving/copying class file. Usually, we use commands like `mktexlsr` or `texhash` depending upon the distribution and operating system.

3. Front matter

The author names and affiliations could be formatted in two ways:

(1) Group the authors per affiliation.
(2) Use footnotes to indicate the affiliations.

See the front matter of this document for examples. You are recommended to conform your choice to the journal you are submitting to.

4. Bibliography styles

There are various bibliography styles available. You can select the style of your choice in the preamble of this document. These styles are Elsevier styles based on standard styles like Harvard and Vancouver. Please use BibTeX to generate your bibliography and include DOIs whenever available.

5. Floats

Figures may be included using the command, `\includegraphics` in combination with or without its several options to further control graphic. `\includegraphics` is provided by graphic[s,x].sty which is part of any standard LaTeX distribution. graphicx.sty is loaded by default. LaTeX accepts figures in the postscript format while pdfLaTeX accepts *.pdf, *.mps (metapost), *.jpg and *.png formats. pdfLaTeX does not accept graphic files in the postscript format.

The `table` environment is handy for marking up tabular material. If users want to use multirow.sty, array.sty, etc., to fine control/enhance the tables, they are welcome to load any package of their choice and cas-sc.cls will work in combination with all loaded packages.

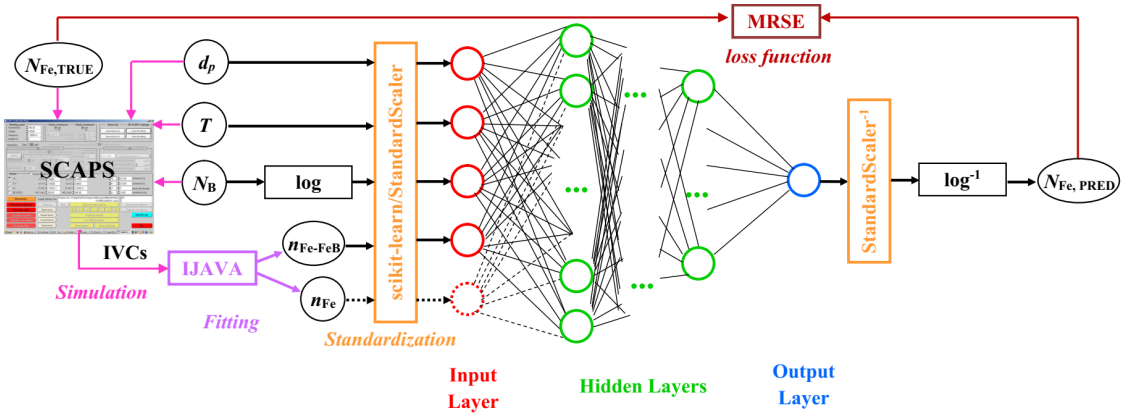

Figure 1: Flowchart of the work steps. Additional details are discussed in the body of the article.

Table 1
This is a test caption. This is a test caption. This is a test caption. This is a test caption.

Col 1	Col 2	Col 3	Col4
12345	12345	123	12345
12345	12345	123	12345
12345	12345	123	12345
12345	12345	123	12345
12345	12345	123	12345

6. Theorem and theorem like environments

cas-sc.cls provides a few shortcuts to format theorems and theorem-like environments with ease. In all commands the options that are used with the `\newtheorem` command will work exactly in the same manner. cas-sc.cls provides three commands to format theorem or theorem-like environments:

```
\newtheorem{theorem}{Theorem}
\newtheorem{lemma}[theorem]{Lemma}
\newdefinition{rmk}{Remark}
\newproof{pf}{Proof}
\newproof{pot}{Proof of Theorem \ref{thm2}}
```

The `\newtheorem` command formats a theorem in LaTeX's default style with italicized font, bold font for theorem heading and theorem number at the right hand side of the theorem heading. It also optionally accepts an argument which will be printed as an extra heading in parentheses.

```
\begin{theorem}
 For system (8), consensus can be achieved with
 $\|T_{\omega z}$ ...
   \begin{eqnarray}\label{10}
   ....
   \end{eqnarray}
\end{theorem}
```

Theorem 1. *For system (8), consensus can be achieved with* $\|T_{\omega z}$ ...

$$....\tag{8}$$

The \newdefinition command is the same in all respects as its \newtheorem counterpart except that the font shape is roman instead of italic. Both \newdefinition and \newtheorem commands automatically define counters for the environments defined.

The \newproof command defines proof environments with upright font shape. No counters are defined.

7. Enumerated and Itemized Lists

cas-sc.cls provides an extended list processing macros which makes the usage a bit more user friendly than the default LaTeX list macros. With an optional argument to the \begin{enumerate} command, you can change the list counter type and its attributes.

```
\begin{enumerate}[1.]
\item The enumerate environment starts with an optional
  argument ‘1.’, so that the item counter will be suffixed
  by a period.
\item You can use ‘a)’ for alphabetical counter and ’(i)’ for
  roman counter.
 \begin{enumerate}[a)]
   \item Another level of list with alphabetical counter.
   \item One more item before we start another.
   \item One more item before we start another.
   \item One more item before we start another.
   \item One more item before we start another.
```

Further, the enhanced list environment allows one to prefix a string like ‘step’ to all the item numbers.

```
\begin{enumerate}[Step 1.]
 \item This is the first step of the example list.
 \item Obviously this is the second step.
 \item The final step to wind up this example.
\end{enumerate}
```

8. Cross-references

In electronic publications, articles may be internally hyperlinked. Hyperlinks are generated from proper cross-references in the article. For example, the words Fig. 1 will never be more than simple text, whereas the proper cross-reference \ref{tiger} may be turned into a hyperlink to the figure itself: Fig. 1. In the same way, the words Ref. [1] will fail to turn into a hyperlink; the proper cross-reference is \cite{Knuth96}. Cross-referencing is possible in LaTeX for sections, subsections, formulae, figures, tables, and literature references.

9. Bibliography

Two bibliographic style files (*.bst) are provided — model1-num-names.bst and model2-names.bst — the first one can be used for the numbered scheme. This can also be used for the numbered with new options of natbib.sty. The second one is for the author year scheme. When you use model2-names.bst, the citation commands will be like \citep, \citet, \citealt etc. However when you use model1-num-names.bst, you may use only \cite command.

thebibliography environment. Each reference is a \bibitem and each \bibitem is identified by a label, by which it can be cited in the text:

In connection with cross-referencing and possible future hyperlinking it is not a good idea to collect more that one literature item in one \bibitem. The so-called Harvard or author-year style of referencing is enabled by the LaTeX package natbib. With this package the literature can be cited as follows:

- Parenthetical: \citep{WB96} produces (Wettig & Brown, 1996).
- Textual: \citet{ESG96} produces Elson et al. (1996).

- An affix and part of a reference: `\citep[e.g.][Ch. 2]{Gea97}` produces (e.g. Governato et al., 1997, Ch. 2).

In the numbered scheme of citation, `\cite{<label>}` is used, since `\citep` or `\citet` has no relevance in the numbered scheme. natbib package is loaded by cas-sc with `numbers` as default option. You can change this to author-year or harvard scheme by adding option `authoryear` in the class loading command. If you want to use more options of the natbib package, you can do so with the `\biboptions` command. For details of various options of the natbib package, please take a look at the natbib documentation, which is part of any standard LaTeX installation.

A. My Appendix

Appendix sections are coded under `\appendix`.

`\printcredits` command is used after appendix sections to list author credit taxonomy contribution roles tagged using `\credit` in frontmatter.

CRediT authorship contribution statement

Oleg Olikh: Conceptualization, Methodology, Formal analysis, Data Curation, Writing - Review & Editing, Visualization, Supervision. **Oleg Lozitsky:** Software, Validation, Investigation, Writing - Original Draft. **Oleksii Zavhorodnii:** Software, Validation, Formal analysis, Writing - Original Draft.

Acknowledgment

This work was supported by National Research Foundation of Ukraine (project number 2020.02/0036)

References

[1] H. Zhu, X. Yu, X. Zhu, Y. Wu, J. He, J. Vanhellemont, D. Yang, Low temperature iron gettering by grown-in defects in p–type Czochralski silicon, Superlattices Microstruct. 99 (2016) 192–196.

[2] C. Claeys, E. Simoen, Metal Impurities in Silicon- and Germanium-Based Technologies: Origin, Characterization, Control, and Device Impact, volume 270 of *Springer Series in Materials Science*, Springer International Publishing, Berlin/New York, 2018.

[3] J. Schmidt, Effect of dissociation of iron–boron pairs in crystalline silicon on solar cell properties, Progress in Photovoltaics: Research and Applications 13 (2005) 325–331.

[4] M. Schubert, M. Padilla, B. Michl, L. Mundt, J. Giesecke, J. Hohl-Ebinger, J. Benick, W. Warta, M. Tajima, A. Ogura, Iron related solar cell instability: Imaging analysis and impact on cell performance, Sol. Energy Mater. Sol. Cells 138 (2015) 96–101.

[5] D. K. Schroder, Semiconductor Material and Device Characterization, John Wiley & Sons, New Jersey, third edition, 2006.

[6] R. C. Kurchin, J. R. Poindexter, V. Vähänissi, H. Savin, C. del Cañizo, T. Buonassisi, How much physics is in a current-voltage curve? inferring defect properties from photovoltaic device measurements, IEEE J. Photovolt. 10 (2020) 1532–1537.

[7] A. R. Peaker, V. P. Markevich, J. Coutinho, Tutorial: Junction spectroscopy techniques and deep-level defects in semiconductors, J. Appl. Phys. 123 (2018) 161559.

[8] S. V. Bulyarskiy, A. V. Lakalin, M. A. Saurov, G. G. Gusarov, The effect of vacancy-impurity complexes in silicon on the current-voltage characteristics of p-n junctions, J. Appl. Phys. 128 (2020) 155702.

[9] S. V. Bulyarskiy, The effect of electron-phonon interaction on the formation of reverse currents of p-n-junctions of silicon-based power semiconductor devices, Solid-State Electron. 160 (2019) 107624.

[10] C. Claeys, E. Simoen, Device performance as a metrology tool to detect metals in silicon, physica status solidi (a) 216 (2019) 1900126.

[11] E. Simoen, C. Claeys, J. Vanhellemont, Defect analysis in semiconductor materials based on p-n junction diode characteristics, in: Defects and Diffusion in Semiconductors - An Annual Retrospective IX, volume 261 of *Defect and Diffusion Forum*, Trans Tech Publications Ltd, 2007, pp. 1–24.

[12] O. Olikh, Relationship between the ideality factor and the iron concentration in silicon solar cells, Superlattices Microstruct. 136 (2019) 106309.

[13] A. S. H. van der Heide, A. Schonecker, J. H. Bultman, W. C. Sinke, Explanation of high solar cell diode factors by nonuniform contact resistance, Progress in Photovoltaics: Research and Applications 13 (2005) 3–16.

[14] L. Duan, H. Yi, C. Xu, M. B. Upama, M. A. Mahmud, D. Wang, F. H. Shabab, A. Uddin, Relationship between the diode ideality factor and the carrier recombination resistance in organic solar cells, IEEE Journal of Photovoltaics 8 (2018) 1701–1709.

[15] J. Chen, M. Zhu, X. Lu, X. Zou, Electrical characterization of GaN Schottky barrier diode at cryogenic temperatures, Appl. Phys. Lett. 116 (2020) 062102.

[16] P. Dalapati, N. Manik, A. Basu, Analysis of the temperature dependence of diode ideality factor in InGaN-based UV-A light-emitting diode, Semiconductors 54 (2020) 1284–1289.

[17] P. Calado, D. Burkitt, J. Yao, J. Troughton, T. M. Watson, M. J. Carnie, A. M. Telford, B. C. O'Regan, J. Nelson, P. R. Barnes, Identifying dominant recombination mechanisms in perovskite solar cells by measuring the transient ideality factor, Phys. Rev. Applied 11 (2019) 044005.

[18] G. Carleo, I. Cirac, K. Cranmer, L. Daudet, M. Schuld, N. Tishby, L. Vogt-Maranto, L. Zdeborová, Machine learning and the physical sciences, Rev. Mod. Phys. 91 (2019) 045002.
[19] S. Ju, S. Shimizu, J. Shiomi, Designing thermal functional materials by coupling thermal transport calculations and machine learning, J. Appl. Phys. 128 (2020) 161102.
[20] S. Rodrigues, H. G. Ramos, F. Morgado-Dias, Machine learning pv system performance analyser, Prog. Photovoltaics Res. Appl. 26 (2018) 675–687.
[21] S. Ju, S. Shimizu, J. Shiomi, Designing thermal functional materials by coupling thermal transport calculations and machine learning, J. Appl. Phys. 128 (2020) 161102.